Inorg. Chem. **2008**, *47*, 6578−6580

Temperature- and Stoichiometry-Controlled Dimensionality in a Magnesium 4,5-Imidazoledicarboxylate System with Strong Hydrophilic Pore Surfaces

K. L. Gurunatha,[†] Kazuhiro Uemura,[‡] and Tapas Kumar Maji*,[†]

Chemistry and Physics of Materials Unit, Jawaharlal Nehru Centre for Advanced Scientific Research, Jakkur, Bangalore 560 064, India, and Graduate School of Science and Engineering, Yamaguchi University, Tokiwadai 2-16-1, Ube-shi 755-8611, Japan

Received April 27, 2008

1D, 2D, and 3D three metal−organic hybrid frameworks of Mg^{II} have been synthesized using 4,5-imidazoledicarboxylic acid (H_3idc) with control of the temperature and stoichiometry in a hydrothermal technique. All of the frameworks show high thermal stability, and frameworks 1D and 3D provide highly hydrophilic pore surfaces, correlated by the selective sorption of water molecules over the organic vapor and other gases like N_2 and CO_2.

Recent years have witnessed an explosion in the synthesis of versatile metal−organic hybrid frameworks with different functionality, exploiting the bridging potential of different organic linkers and geometry of the metal ions.[1] Hybrid solids with different topology and dimensionality constructed from the same building unit provide versatile functionality.[2] For the desired framework and functionality in a hybrid solid, it is important to control and understand the external factors, such as pH, temperature, and solvent, that govern the crystallization process and the stability of the overall crystals.[2,3] Cheetham et al. reported the temperature-controlled different dimensionality and topology in a cobalt succinate system.[3a] Later on, Stock et al., Li et al., and others showed that the high reaction temperature and pH increase the dimensionality and formation of M−O−M linkages.[3b–h] Recently, 4,5-imidazoledicarboxylic acid (H_3idc) and 3,5-pyrazoledicarboxylic acid (H_3pdc) were used to synthesize various functional metal−organic hybrid frameworks.[3f,4,5] Both ligands have three pH-dependent abstractable protons and six donor sites, which can be exploited for the synthesis of a variety of hybrid solids through a number of flexible binding modes. Of more significance, the spatial disposition of the two N atoms in H_3idc with a N−X−N angle of about 144° (X = center of the imide ring), similar to the Si−O−Si angle in zeolite, may provide a porous zeolite-like network.[4a] Moreover, porous solids with alkali or alkaline-earth metals are attractive because of their small density, and that makes them potential candidates for hydrogen and methane storage materials.[3d,6,7] Among the s-block metals, the large polarizing power of Mg^{II} can provide a strong coordination bond with

* To whom correspondence should be addressed. E-mail: tmaji@jncasr.ac.in.
† Jawaharlal Nehru Centre for Advanced Scientific Research.
‡ Yamaguchi University.

(1) (a) Kitagawa, S.; Kitaura, R.; Noro, S.-I. *Angew. Chem., Int. Ed.* **2004**, *43*, 2334. (b) Yaghi, O. M.; O'Keeffe, M.; Ockwig, N. W.; Chae, H. K.; Eddaoudi, M.; Kim, J. *Nature* **2003**, *423*, 705. (c) Janiak, C. *Dalton Trans.* **2003**, 2781. (d) Rao, C. N. R.; Natarajan, S.; Vaidhyanathan, R. *Angew. Chem., Int. Ed.* **2004**, *43*, 1466. (e) Férey, G. *Chem. Soc. Rev.* **2008**, *37*, 191.

(2) (a) Moulton, B.; Zaworotko, M. J. *Chem. Rev.* **2001**, *101*, 1629. (b) Bradshaw, D.; Claridge, J. B.; Cussen, E. J.; Prior, T. J.; Rosseinsky, M. J. *Acc. Chem. Res.* **2005**, *38*, 273. (c) Holmes, K. E.; Kelly, P. F.; Elsegood, M. R. J. *Dalton Trans.* **2004**, 3488.

(3) (a) Forster, P. M.; Burbanki, A. R.; Livage, C.; Férey, G.; Cheetham, A. K. *Chem. Commun.* **2004**, 368. (b) Stock, N.; Bein, T. *J. Mater. Chem.* **2005**, *15*, 1384. (c) Forster, P. M.; Stock, N.; Cheetham, A. K. *Angew. Chem., Int. Ed.* **2005**, *44*, 7608. (d) Livage, C.; Egger, C.; Nogues, M.; Férey, G. *J. Mater. Chem.* **1998**, *8*, 2743. (e) Livage, C.; Egger, C.; Férey, G. *Chem. Mater.* **2001**, *13*, 410. (f) Pan, L.; Frydel, T.; Sander, M. B.; Huang, X.; Li, J. *Inorg. Chem.* **2001**, *40*, 1271. (g) Tong, M.-L.; Kitagawa, S.; Chang, H.-C.; Ohba, M. *Chem. Commun.* **2004**, 418. (h) Fang, R.-Q.; Zhang, X.-M. *Inorg. Chem.* **2006**, *45*, 4801.

(4) (a) Maji, T. K.; Mostafa, G.; Chang, H.-C.; Kitagawa, S. *Chem. Commun.* **2005**, 2436. (b) Gu, J.-Z.; Lu, W.-G.; Jiang, L.; Zhou, H.-C.; Lu, T.-B. *Inorg. Chem.* **2007**, *46*, 5837. (c) Lu, W. G.; Su, C. Y.; Lu, T. B.; Jiang, L.; Chen, J. M. *J. Am. Chem. Soc.* **2006**, *128*, 34. (d) Liu, Y. L.; Kravtsov, V.; Larsen, R.; Eddaoudi, M. *Chem. Commun.* **2006**, 1488. (e) Sun, Y. Q.; Zhang, J.; Yang, G. Y. *Chem. Commun.* **2006**, *n/a*, 4700. (f) Fang, R. Q.; Zhang, X. M. *Inorg. Chem.* **2006**, *45*, 4801.

(5) (a) Pan, L.; Huang, X.; Li, J.; Wu, Y.; Zheng, N. *Angew. Chem., Int. Ed.* **2000**, *39*, 527. (b) King, P.; Clérac, R.; Anson, C. E.; Powell, A. K. *Dalton Trans.* **2004**, *n/a*, 852.

(6) (a) Côté, A. P.; Shimizu, G. K. H. *Chem.−Eur. J.* **2003**, *9*, 5361. (b) Son, S. U.; Reingold, J. A.; Kim, S. B.; Carpenter, G. B.; Sweigart, D. A. *Angew. Chem., Int. Ed.* **2005**, *44*, 7710. (c) de Lill, D. T.; Bozzuto, D. J.; Cahill, C. L. *Dalton Trans.* **2005**, 2111. (d) Richards, P. I.; Benson, M. A.; Steiner, A. *Chem. Commun.* **2003**, 1392.

(7) (a) Davies, R. P.; Less, R. J.; Lickiss, P. D.; White, A. J. P. *Dalton Trans.* **2007**, 2528. (b) Dincă, M.; Long, J. R. *J. Am. Chem. Soc.* **2005**, *127*, 9376. (c) Senkovska, I.; Kaskel, S. *Eur. J. Inorg. Chem.* **2006**, 4564. (d) Rood, J. A.; Noll, B. C.; Henderson, K. W. *Inorg. Chem.* **2006**, *45*, 5521. (e) Williams, C. A.; Blake, A. J.; Wilson, C.; Hubberstey, P.; Schröder, M. *Cryst. Growth Des.* **2008**, *8*, 911. (f) Zhang, J.; Chen, S.; Valle, H.; Wong, M.; Austria, C.; Cruz, M.; Bu, X. *J. Am. Chem. Soc.* **2007**, *129*, 14168. (g) Rood, J. A.; Boggess, W. C.; Noll, B. C.; Henderson, K. W. *J. Am. Chem. Soc.* **2007**, *129*, 13675.

10.1021/ic8007377 CCC: $40.75
Published on Web 07/11/2008

Scheme 1. Schematic Diagram of the Synthetic Conditions for **1**−**3**, with the Right Side Showing the Binding Mode of the H_3idc Ligand in the Respective Framework

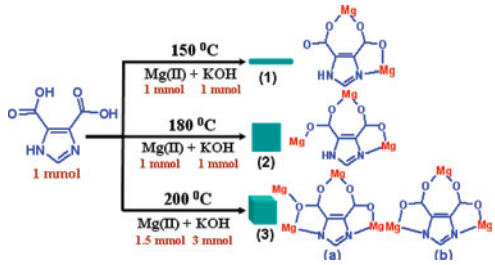

oxygen, and there are very few porous hybrid frameworks based on Mg^{II} that have been reported.[7] In this Communication, we report temperature- and stoichiometry-controlled hydrothermal syntheses (Scheme 1), structural characterizations, and porous properties of three lightweight hybrid frameworks, 1D $\{[Mg(Hidc)(H_2O)_2]\cdot 1.5H_2O\}_n$ (**1**), 2D $[Mg(Hidc)(H_2O)]_n$ (**2**), and 3D $\{[Mg_3(idc)_2(H_2O)_5]\cdot 2H_2O\}_n$ (**3**) (H_3idc = 4, 5-imidazoledicarboxylic acid).

IR spectra of **1**−**3** (Figures S1−S3 in the Supporting Information (SI)) show broad bands in the region of 3100−3500 cm^{-1}, suggesting the presence of H_2O molecules.[8] The $\nu_{sym}(CO_2)$ was observed at lower frequencies, 1410−1505 cm^{-1}, with a $\Delta\nu$ value of 95−100 cm^{-1} indicating the bidentate chelate coordination mode of Hidc/idc in **1**−**3**.[8]

Compound **1** crystallizes in the monoclinic *C*2/*c* space group,[9a] and structural determination reveals a 1D coordination chain of Mg^{II} linked by Hidc (Figure 1a). In the chain, each Hidc ligand chelated to two Mg^{II} centers via N1,O4 and O3,O5 and the octahedral geometry around Mg^{II} is fulfilled by the two coordinated water molecules (O1 and O2; Figure 1a). Therefore, Hidc ligand acts as a dianioinc and bridging bichelating ligand (Scheme 1). Mg−O bond distances are in the range of 2.0117(17)−2.1487(18) Å, and the Mg−N1 bond distance is 2.146(2) Å. 1D chains are engaged in hydrogen-bonding interactions with coordinate water molecule O1 and carboxylate oxygens O5 and O6 [O1···O6 = 2.958(2) Å and O1···O5 = 3.038(2) Å], forming a 2D supramolecular sheet in the *bc* plane (Figure S4 in the SI). 2D sheets are further linked by hydrogen bonds through uncoordinated imidazole nitrogen N2 and the pendent carboxylate oxygen O6 [N1···O6 = 2.785(2) Å], forming a 3D surpramolecular framework with 1D channels occupied by the water molecules along the crystallographic

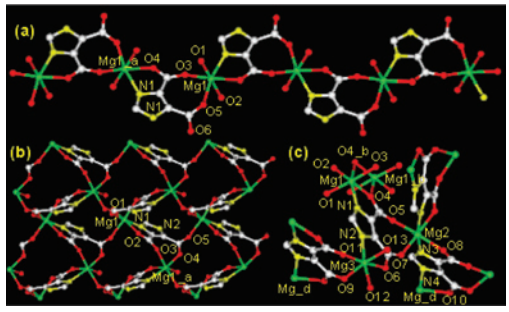

Figure 1. Coordination environment around Mg^{II} in (a) **1** (symmetry code: a = $^3/_2 - x$, $^1/_2 + y$, $^1/_2 - z$), (b) **2** (a = x, y, $1 + z$), and (c) **3** (b = $3 - x$, $1 - y$, $-z$; d = $^1/_2 + x$, $^1/_2 - y$, $^1/_2 + z$).

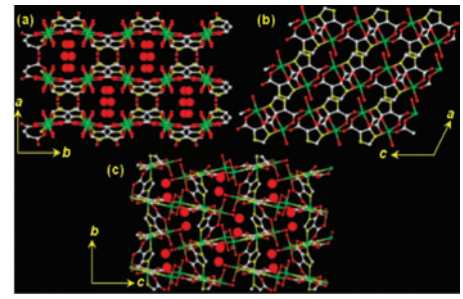

Figure 2. Overall structures of (a) the 3D supramolecular framework of **1** with 1D water-filled channels along the *c* axis, (b) 2D sheets in **2** stacked along the *b* axis with hydrogen-bonding interactions forming the 3D hydrogen-bonded framework, and (c) the 3D coordination framework of **3** with 1D water-filled dumbbell-shaped channels along the *a* axis.

c axis (Figure 2a). The guest water molecules are hydrogen-bonded to each other [O7···O8 = 2.819(2) Å] and further connected with the coordinated water molecule O2, forming a cyclic hexagonal arrangement of the water molecules (Figure S5 in the SI). The void space was calculated using *PLATON*,[10] suggesting a 12.9% void volume to the total crystal volume; however, this would be increased to 29.6% after removal of the coordinated water molecules. The effective hexagonal pore size considering the van der Waals radii is 4.5 × 4.5 $Å^2$ (Figure S6(a) in the SI).[11a]

Changing the temperature from 160 to 180 °C for the same reaction mixture of **1** affords compound **2** (SI), which crystallizes in the monoclinic chiral $P2_1$ space group.[9b] Structural determination reveals that each Hidc ligand is chelated to two different Mg^{II} centers through N1,O2 and O3,O4 and connected to another Mg^{II} via monodentate carboxylate oxygen O5, forming a 2D sheet in the crystallographic *bc* plane (Figure 1b and Scheme 1). Each Mg^{II} is coordinated to one water molecule (O1) and fulfills the octahedral geometry. Mg−O bond distances are in the range of 2.037(2)−2.112(3) Å, and the Mg−N1 bond distance is 2.189(4) Å, slightly higher than that of **1**. In between the 2D sheets, the coordinated water molecule O1 and imidazole nitrogen atom N2 are involved in hydrogen bonding with the carboxylate oxygen atoms O3 and O5 [O···O = 2.8663(18)−2.729(2) Å; O···N = 2.946(2) Å], forming a 3D supramolecular network (Figures 2b and S6(b) in the SI).

With an increase in the metal concentration, pH, and temperature to 200 °C, square-block crystals of **3** are obtained quantitatively (SI). Compound **3** crystallizes in the mono-

(8) Nakamoto, K. *Infrared and Raman Spectra of Inorganic and Coordination Compounds*, 5th ed.; John Wiley & Sons: New York, 1997.
(9) (a) Crystal data of **1**: $C_5H_9MgN_2O_{7.5}$, M_r = 241.45, monoclinic, *C*2/*c* (No. 15), a = 13.9242(4) Å, b = 11.6256(3) Å, c = 12.0761(3) Å, β = 108.240(1)°, V = 1856.62(9) $Å^3$, Z = 8, obsd data [$I > 2\sigma(I)$] = 1390, R = 0.0338, R_w = 0.0945, GOF = 1.04. (b) Crystal data of **2**: $C_5H_4MgN_2O_5$, M_r = 196.41, monoclinic, $P2_1$ (No. 4), a = 7.0347(2) Å, b = 7.4802(2) Å, c = 7.3586(3) Å, β = 117.965(1)°, V = 342.00(2) $Å^3$, Z = 2, obsd data [$I > 2\sigma(I)$] = 1740, R = 0.0289, R_w = 0.0744, GOF = 1.04, Flack parameter = 0.5. (c) Crystal data of **3**: $C_{10}H_{16}Mg_3N_4O_{15}$, M_r = 505.20, monoclinic, $P2_1/n$ (No. 14), a = 10.4503(7) Å, b = 16.6457(11) Å, c = 11.4380(8) Å, β = 108.225(3)°, V = 1889.9(2) $Å^3$, Z = 4, obsd data [$I > 2\sigma(I)$] = 2310, R = 0.0248, R_w = 0.0660, GOF = 1.04.
(10) Spek, A. L. *PLATON*; The University of Utrecht: Utrecht, The Netherlands, 1999.
(11) (a) The size is measured by considering van der Waals radii for constituting atoms. (b) Beck, D. W. *Zeolite Molecular Sieves*; John Wiley & Sons: New York, 1974.

clinic $P2_1/n$ space group,[9c] and the asymmetric unit comprises three Mg^{II} centers. Each octahedral Mg1 is attached to one chelated idc via N1,O4 and another idc through the monodentate carboxylate oxygen O4_b, and the remaining three sties are occupied by the water molecules O1, O2, and O3 (Figure 1c), whereas the octahedral Mg2 is coordinated to the three different chelated idc. Two chelated idc via N2,O6 and O9,O11 and two water molecules O12 and O13 form the octahedral coordination around Mg3. The Mg−O and Mg−N bond distances are in the range of 2.0215(16)−2.124(2) and 2.103(2)−2.1647(17) Å, respectively. In framework **3**, one idc ligand functions as a tetradentate ligand and another one acts as a tridentate ligand (Scheme 1), forming the overall 3D network. The resultant 3D network contains a 1D channel along the crystallographic *a* axis occupied by the four water molecules (Figure 2c). The potential solvent-accessible void volume suggests 4.0% and 26.2% void space to the total crystal volume after removal of the guest as well as the coordinated water molecules, respectively. The dehydrated framework shows an irregular dumbbell-shaped channel with a dimension of 3.0 × 8.6 $Å^2$ (Figure S6(c) in the SI).

Thermogravimetric analysis (TGA) of all three compounds is shown in Figure S7 in the SI. In the case of framework **1**, 18.6% weight loss was observed between 50–135 °C, corresponding to the guest and one coordinated water molecule (obsd 18.7%). Then another coordinated water molecule is released at 220 °C (calcd 6.97 wt %; obsd 6.99 wt %) to give $[Mg(Hidc)]_n$ (**1′**). For compound **2**, the coordinated water molecule was liberated between 250–300 °C and the dehydrated framework is stable up to 385 °C. TGA for **3** shows stepwise weight loss of the guest and coordinated water molecules in the temperature range of 70−355 °C and dehydrated framework $[Mg_3(idc)_2]_n$ (**3′**) is stable up to 500 °C. Figure S8 in the SI shows powder X-ray diffraction (PXRD) patterns of the as-synthesized **1** and the dehydrated framework **1′**, exhibiting changes in peak positions and intensities and the emergence of some new peaks. Similarly, as shown in Figure S9 in the SI, the PXRD pattern of the dehydrated framework **3′** shows a shifting of peak positions and the appearance of some new peaks compared to the original **3**. These observations suggest that significant rearrangement occurs in the as-synthesized framework of **1** and **3** and ultimately leads to a pore structure with coordinatively unsaturated Mg^{II} centers lying on the pore surface.

To confirm the permanent porosity and selectivity, sorption analyses were carried out using the dehydrated samples **1′** and **3′**. Figures S10 and S11 in the SI showing sorption of N_2 (kinetic diameter, 3.6 Å)[11b] at 77 K and CO_2 (3.4 Å) at 195 K for **1′** and **3′**, respectively, exhibit type III sorption profiles, suggesting only surface adsorption. This may be attributed to the smaller channel aperture after dehydration compared to the kinetic diameters of N_2 and CO_2.[7b] We have also measured the sorption properties with MeOH (4.0 Å) and H_2O (2.65 Å) vapor at 298 K, which is shown in Figures S12 in the SI and 3, respectively. Framework **1′** shows a type II sorption profile with MeOH and about 0.18 molecule of MeOH included per formula unit. This is also consistent with the different PXRD patterns with MeOH compared to those of **1′** (Figure S8(f) in the SI). On the other hand, framework **3′** does not uptake any MeOH, which is also supported by the PXRD patterns similar to those of the dehydrated sample (Figure S9(g) in the SI). The H_2O sorption profile of **1′** (Figure 3) reveals a gradual uptake up to $P/P_0 = 0.36$ and then a steep uptake up to $P/P_0 = 0.54$ with a small step at $P/P_0 = 0.44$. Then this gradually increases with pressure and reaches an amount of 289 mL/g at $P/P_0 = 0.95$, which corresponds to 2.3 molecules of H_2O per formula unit, whereas **3′** shows a gradual uptake of H_2O with increasing pressure and without any step and reaches an amount of 142 mL/g at $P/P_0 = 0.96$, suggesting 2.4 molecules of H_2O per formula unit. Both of the profiles were analyzed by the Dubinin−Radushkevich equation, and the values of βE_0 are 9.68 (**1′**) and 6.92 (**3′**) kJ/mol, which reflect the adsorbate−adsorbent affinity, indicating that **1′** is rather more hydrophilic than **3′**. Stepwise sorption, stronger affinity, and high uptake of H_2O in **1′** would be due to the effective pore size, shape, and different adsorption sites, which are unlike those from **3′**. In the case of **1′**, regular hexagonal 1D channels are aligned with the four unsaturated Mg^{II} centers, whereas in the case of **3′**, the unsaturated Mg^{II} sites are in a more diffused state in the smaller irregular dumbbell-shaped pores. Therefore, in **3′**, H_2O molecules cannot interact directly with Mg^{II} centers, resulting in the smaller uptake. In both cases, structural reversal with water vapor was correlated by the PXRD patterns (Figures S8 and S9 in the SI).

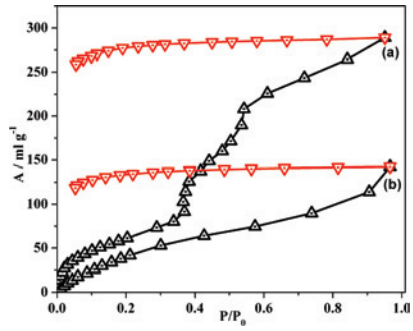

Figure 3. H_2O sorption isotherms at 298 K (black, adsorption; red, desorption): (a) for **1′**; (b) for **3′**. (P_0 is the saturated vapor pressure of H_2O at 298 K).

In conclusion, we have synthesized 1D, 2D, and 3D Mg^{II} frameworks using the H_3idc ligand by controlling the temperature and stoichiometry. All of the frameworks show high thermal stability conferred by the strong Mg−O bonds. The dehydrated **1′** and **3′** exhibit highly selective sorption properties to H_2O over N_2 or CO_2. Frameworks **1′** and **3′** unveil a very strong hydrophilic character, and they may find application in the separation of hydrophilic and hydrophobic molecules.

Acknowledgment. T.K.M. is grateful to the DST for financial support (fast track proposal).

Supporting Information Available: Details of the experimental procedure, Figures S1−S13, Tables S1−S6, and X-ray crystallographic files in CIF format for **1**−**3**. This material is available free of charge via the Internet at http://pubs.acs.org.

IC8007377